Heliyon 9 (2023) e20205

Contents lists available at ScienceDirect

Heliyon

journal homepage: www.cell.com/heliyon

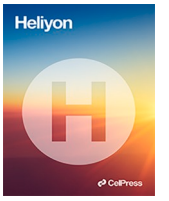

Effectiveness of silver nitrate application on plant growth and bioactive compounds in *Agastache rugosa* (Fisch. & C.A. Mey.) kuntze

Vu Phong Lam [a,c,1], Lee Beomseon [e,1], Vu Ky Anh [b], Dao Nhan Loi [b,c], Sunwoo Kim [b], Lee Kwang-ya [d], Jongseok Park [a,b,*]

[a] *Department of Horticultural Science, Chungnam National University, Daejeon, 34134, South Korea*
[b] *Department of Bio-AI Convergence, Chungnam National University, Daejeon, 34134, South Korea*
[c] *Department of Agronomy, Tay Bac University, Son La, 360000, Viet Nam*
[d] *Institude of Agriculture Science, Chungnam National University, Daejeon, 34134, South Korea*
[e] *Naru Agricultural Consultancy Company, Jisanmaeul-gil 19, Buk-gu, Gwangju city, 61014, South Korea*

ARTICLE INFO

Keywords:
Acacetin
Chlorophyll
Hydroponic
Rosmarinic acid
Tilianin

ABSTRACT

The objective of this study was to determine the optimal dose of silver nitrate ($AgNO_3$) for plant growth and to increase the main bioactive compounds in *A. rugosa* cultivated in a hydroponic system. The application of soaked diniconazole (120 μmol mol^{-1}) to all plants at 7 days after transplanting (DAT) for dwarfing plant height, optimizing cultivation space in the plant factory. Subsequently, plants were soaked with 50, 100, 200, and 400 μmol mol^{-1} $AgNO_3$ for 10 min at 25 DAT and harvested at 39 DAT. The results indicated that 200 and 400 μmol mol^{-1} treatments tended to severely decrease plant growth parameters compared to treatments with lower concentrations. The net photosynthetic rate was significantly reduced by the 200 and 400 μmol mol^{-1} treatments compared to treatments with other concentrations. The 400 μmol mol^{-1} treatment led to the lowest concentrations of chlorophyll *a*, chlorophyll *a*/b, total carotenoid, chlorophyll *b*, and the total chlorophyll. However, 2,2-diphenyl-1-picrylhydrazyl (DPPH) radical scavenging activity was considerably increased in 50, 100, 200, and 400 μmol mol^{-1} compared to that of the control plants. A higher rosmarinic acid (RA) concentration in the whole plant was noticed with the 400 μmol mol^{-1} treatment compared with that of the untreated plants. The 100 μmol mol^{-1} treatment exhibited the highest concentration and content of tilianin in the whole plant. Concentration of acacetin 1 significantly increased in the whole plant with 100 and 200 μmol mol^{-1} treatments compared with that of the untreated plants. Concentrations of acacetin 2 and 3 in the whole plant were the highest with 100 and 200 μmol mol^{-1} treatments, respectively. The results demonstrated that 100 μmol mol^{-1} treatments can be used to increase bioactive compounds without severely limiting the plant growth and reducing chlorophyll concentrations of *A. rugosa*. Implementing this optimal dose can enable growers and researchers to cultivate *A. rugosa* more efficiently, enhancing bioactive compound content and overall plant performance, thus harnessing the potential health benefits of this valuable plant species.

* Corresponding author. Department of Horticultural Science, Chungnam National University, Daejeon, 34134, South Korea.
E-mail address: jongseok@cnu.ac.kr (J. Park).
[1] These authors contributed equally to this work.

https://doi.org/10.1016/j.heliyon.2023.e20205
Received 20 June 2023; Received in revised form 7 September 2023; Accepted 13 September 2023
Available online 17 September 2023

1. Introduction

The Lamiaceae family (mint family) includes more than 7000 species distributed throughout subtropical, tropical, and temperate regions worldwide [1]. *Agastache rugosa* is a member of the mint family [2]. The market value of *A. rugosa* is primarily based on its essential oil content and has attracted attention because of its diverse application in pharmaceuticals, culinary, cosmetics, medicine, and food products [2]. This medicinal herb is known for its antioxidant [3], antimicrobial [4], anticancer [5], anti-inflammatory [6], analgesic [7], and cardiovascular properties [8], and is presumed to promote the human immune system response [9]. Plant polyphenols include simple phenols, hydroxybenzoic acids [10], hydroxycinnamic acids [11], and flavonoids such as flavones [12], flavanones [13], and flavonols [14,15]. Among these, the main bioactive compounds in *A. rugosa* are tilianin (an active flavonoid glycoside), acacetin (flavone), and rosmarinic acid (RA) (esters of caffeic acid and 3,4-dihydroxyphenyllactic acid) [16]. Acacetin is a flavone that is used to treat cancers, infections, inflammation, and metabolic disorders [17]. Tilianin has antidiabetic, cardioprotective, antihypertensive, neuroprotective, anti-atherogenic, antidepressant, anti-inflammatory, and antioxidant effects [18]. RA has many pharmacological uses, including antitumorigenic, antioxidative, anti-inflammatory, and anti-apoptotic [19]. The growing concerns regarding the bioactive quality and nutritional value of food sources, alongside the increasing economic and environmental considerations regarding sustainable crop management, underline the need for sustainable, profitable, and ecologically advantageous solutions to increase the quality of *A. rugosa*.

Environmental factors, including light, temperature, humidity, and carbon dioxide (CO_2), are controlled to allow year-round production and to increase plant productivity and quality [20]. Although *A. rugosa* can reach a height of 50–60 cm within 5–6 weeks, making it unsuitable for cultivation in the limited vertical space of a plant factory, we explored the use of diniconazole to reduce its height [21,22]. By controlling the plant height, our goal was to increase the number of cultivation layers in the plant factory, thereby maximizing space utilization and overall productivity. Therefore, this study utilized diniconazole to decrease the height of *A. rugosa* plants. Heavy metal exposure is an abiotic stress that alters primary metabolic processes and plant physiology, including respiration, photosynthesis, yield, plant growth, and secondary metabolites. The effects of silver nitrate ($AgNO_3$) on plants have been studied over the past few decades [23–25]. $AgNO_3$ has been widely applied in fields such as agriculture [23,26], medical science [27], and environmental management [28]. It is primarily used in agriculture to achieve a range of results, such as plant growth and development control, high-quality plants, and flowering control [29–31]. Although the potential of $AgNO_3$ is widely accepted, its use in agriculture to increase secondary metabolite levels in plants remains debated [23]. The influence of $AgNO_3$ on plant growth and secondary metabolites has been explored in crops such as *Bacopa monnieri* [32], *Cucumis sativus* L. [33], *Brassica* sp. [23], and pearl millet [34]. *Brassica* seedling growth decreases due to $AgNO_3$ accumulation, which can severely inhibit photosynthesis. $AgNO_3$ causes oxidative stress, as demonstrated by an increase in hydrogen peroxide and superoxide radicals [23]. The influence of toxic silver is correlated with the accumulation of oxidative damage and reactive oxygen species (ROS). In response, plants operate an antiradical enzymatic system to synthesize small antioxidant compounds [35]. Hydrogen peroxide content, total phenolic compounds, and lipid peroxidation in potatoes were considerably increased under $AgNO_3$ treatment compared with those in untreated explants [36]. Increases in catalase and peroxidase activities and total phenol content under $AgNO_3$ treatments were detected in the leaves, stems, and roots of *Bacopa monnieri* compared to control plants [32].

However, to date, no studies have successfully examined the effects of $AgNO_3$ on plant growth or bioactive compound production in *A. rugosa* plants cultivated using the deep-flow technique in a plant factory. This study aimed to determine the optimal $AgNO_3$ dose to enhance bioactive compound accumulation without severely reducing the plant growth of *A. rugosa* and to suggest cultivation conditions for creating high-quality plants.

2. Materials and methods

2.1. Seedling growing conditions

A. rugosa seeds were obtained from Danong Co. Ltd (Seoul, Korea) and sown on a seed germination tray in an environment-controlled room. The seedling conditions were set up at 21 ± 3 °C with a relative humidity of 75 ± 10% and a photosynthetic photon flux density (PPFD) of 185 ± 15 μmol m^{-2} s^{-1} using a fluorescent lamp (TL5 14 W/865 Philips, Amsterdam, Netherlands) with 16 h of light and 8 h of darkness (16/8) photoperiod. The Hoagland solution with electrical conductivity (EC) 1.1 dS m^{-1} and pH 6.0 was used for seedlings from 2 weeks after sowing.

2.2. Treatments

On day 28 after sowing, seedlings were moved to a deep flow technique system of dimensions 0.11 m × 1.2 m × 0.7 m; H × L × W placed in a plant factory. The cultivation conditions were controlled at an average temperature of 22.5 °C with a relative humidity of 65 ± 10%, 220 ± 10 μmol m^{-2} s^{-1} of PPFD with 14 h of light and 10 h of dark (14/10) photoperiod. The plants were cultivated for 39 d in Hoagland solution with a pH of approximately 6.5 and EC of 2.0 dS m^{-1}. All the plants were treated with diniconazole (120 μmol mol^{-1}) for 10 min by root soaking for dwarfing at 7 d after transplantation (DAT). Four $AgNO_3$ concentrations of 50, 100, 200, and 400 μmol mol^{-1} (control treatment without $AgNO_3$) were treated by soaking the roots at 25 DAT for 10 min.

2.3. Plant growth parameter measurements

Thirty 9 d after transplantation, all samples were harvested. Leaf width, leaf number, stem length, leaf length, leaf area, shoot and root fresh weights/plant, and dry weights of shoots and roots per plant were recorded. Shoots and roots/plant were weighed to determine the fresh weights, then moved to an oven for 1 week at 70 °C, and the dry weights/plant were weighed. Leaves were detached from each plant to determine leaf area. A digital camera (Canon EOS 850D, Canon Inc., Tokyo 146–8501, Japan) and ImageJ software were used to determine leaf area (Fig. 1).

2.4. Photosynthetic activity

Photosynthetic characteristics, including the net photosynthetic rate (P_n; μmol CO_2 m^{-1} s^{-1}), transpiration rate (T_r; mmol H_2O mol^{-1}), intercellular CO_2 concentration (C_i; μmol CO_2 mol^{-1}), and stomatal conductance (g_s; mol H_2O m^{-1} s^{-1}), were determined using a portable photosynthesis system (LICOR 6400, Licor. Inc. Nebraska, NE, USA). Measurements were recorded in a leaf chamber with CO_2 concentration of 400 μmol mol^{-1}, PPFD of 1000 μmol m^{-2} s^{-1}, leaf temperature of 25 °C, and an air flow rate of 500 cm^3 s^{-1}.

2.5. Photosynthetic pigments and 2,2-diphenyl-1-picrylhydrazyl (DPPH) radical scavenging activity

Upon harvesting, the leaves, stems, and flowers of each *A. rugosa* plant replicate were promptly immersed in liquid nitrogen and stored in a deep freezer at −70 °C; subsequently, they were transferred to a dry freezer at −50 °C (TFD5503, IL Shinbiobase Co. Ltd, Gyeonggi-do, Korea) within 4 d. A porcelain mortar and pestle were employed to ground each sample, and the dry powder was filtered through mesh sieves. Twenty milligrams of dry powdered shoots was extracted with 2 mL of 90% MeOH. The obtained extract was centrifuged at 1308×*g* for 20 min. Chlorophyll (Chl) concentrations (Chl a and Chl b), total carotenoids (Car), and DPPH radical scavenging activity were analyzed using an Epoch microplate spectrophotometer (EPOCH-SN, Agilent Technologies, Inc., Santa Clara, CA 95051, USA). Following the method of Lichtenthaler, 1987 and Machado et al., 2020 [37,38], Chl a, Car, and Chl b were detected at 652.4, 470, and 665.2 nm, respectively. The DPPH radical scavenging assay was performed at 517 nm, according to Rahman et al., 2015 [39]. The Chl a, Chl b, Car, DPPH, Chl a and b ratio (Chl a/b), and total Chl a + b concentrations were calculated using the following formulas:

$$\text{Chl a } (mg \cdot g^{-1}) = (16.82 \times A_{665.2} - 9.28 \times A_{652.4})/10$$

$$\text{Chl b } (mg \cdot g^{-1}) = (36.92 \times A_{652.4} - 16.54 \times A_{665.2})/10$$

$$\text{Total carotenoid } (mg \cdot g^{-1}) = [(1000 \times A_{470} - 1.91 \times \text{Chl a} - 95.15 \text{ Chl b})/225]/10$$

$$\text{DPPH } (\%) = (A_{blank} - A_{sample})/A_{blank} \times 100$$

$$\text{Chl a and b ratio (Chl a/b)} = \text{Chl a/Chl b}$$

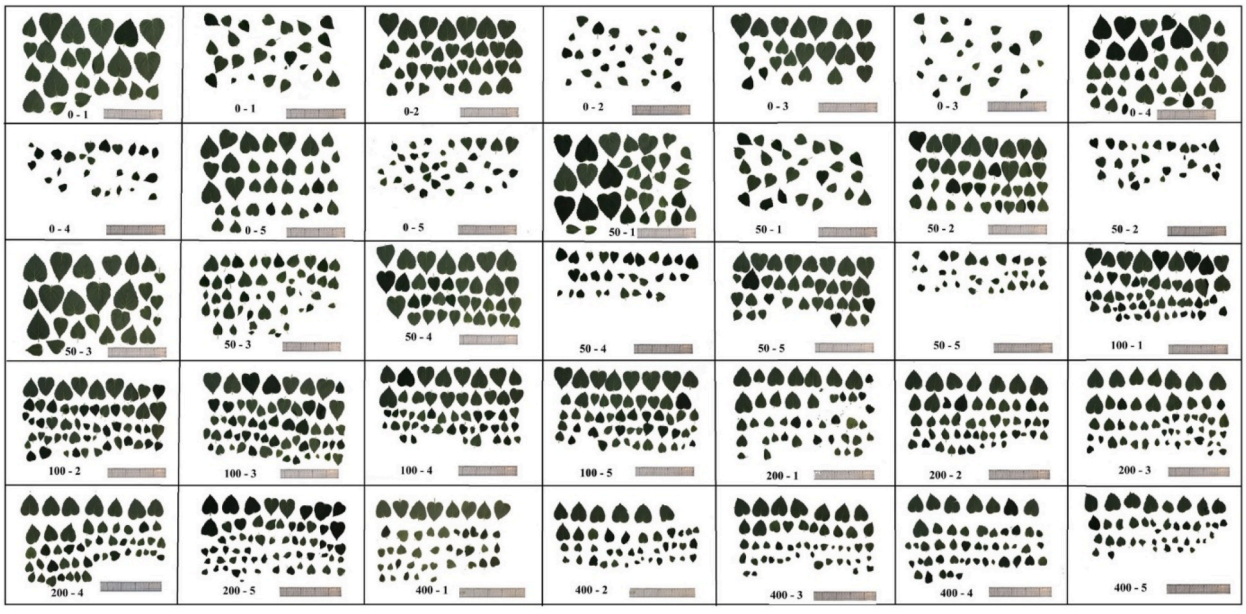

Fig. 1. Representative *A. rugosa* leaf images of the different $AgNO_3$ treatments (0-control, 50 μmol mol^{-1}, 100 μmol mol^{-1}, 200 μmol mol^{-1}, and 400 μmol mol^{-1}) under study. Images are five plants per treatment (n = 5).

Table 1
The growth characteristics of *A. rugosa* at different $AgNO_3$ treatments (0-control, 50 μmol mol^{-1}, 100 μmol mol^{-1}, 200 μmol mol^{-1}, and 400 μmol mol^{-1}), subjected to root soaking.

$AgNO_3^w$ (μmol·mol^{-1})	Leaf length (cm)	Leaf width (cm)	Number of leaves (leaves)	Leaf area (cm^2)	Stem length (cm)	SFWP (g/plant)	RFWP (g/plant)	Root length (cm)	SDWP (g/plant)	RDWP (g/plant)	LDWP (g/plant)	FDWP (g/plant)	Stem DWP (g/plant)
0	6.26a	5.70	56.60 ab	532.67a	20.80a	17.21a	11.24a	77.08a	2.91a	0.87a	1.67	0.65a	0.61 ab
50	6.04 ab	5.64	64.80a	574.76a	18.92 ab	16.65a	11.97a	62.50b	2.62 ab	0.86a	1.40	0.58a	0.63a
100	5.90 ab	5.60	54.40abc	473.34 ab	18.70 ab	13.88 ab	11.37a	61.03b	2.58 ab	0.78 ab	1.50	0.63a	0.46BCE
200	5.64b	5.40	51.80bc	390.67bc	17.62b	11.26bc	7.03b	56.06b	2.58 ab	0.69 ab	1.48	0.53a	0.57 ab
400	5.54b	5.24	45.00c	283.58c	10.66c	8.37c	6.15b	54.96b	1.96b	0.60b	1.25	0.37b	0.34c
Significance[z]	**	NS	***	***	***	***	***	***	**	**	NS	***	***
L[y]	***	***	***	***	***	***	***	***	***	**	*	**	***
Q[x]	***	**	**	***	***	***	***	***	***	**	NS	***	**

[W]$AgNO_3$; NS: not significant ($p > 0.05$); [z]significant at * $p \leq 0.05$, ** $p \leq 0.01$, and *** $p \leq 0.001$; [y]L: linear; [x]Q: quadratic in regression analysis. Values are the means of five samples ($n = 5$). Different letters are significant differences among treatments at $p \leq 0.05$, according to Tukey's test. SFWP: Shoot fresh weight/plant; RFWP: Root fresh weight/plant; SDWP: Shoot dry weight/plant; RDWP: Root dry weight/plant; LDWP: Leaf dry weight/plant; FDWP: Flower dry weight/plant, and stem DWP: Stem dry weight/plant.

Total Chl a + b (mg.g^{-1}) = Chl a + Chl b
where A is the absorbance at wavelength.

2.6. Analyzation of acacetin, tilianin, three acacetin glycosides, and rosmarinic acid concentrations and contents

The roots, stems, leaves, and flowers of *A. rugosa* from each replicate were promptly immersed in liquid nitrogen and stored in a deep freezer at −70 °C; subsequently, they were transferred to a dry freezer at −50 °C (TFD5503, IL Shinbiobase Co. Ltd, Gyeonggi-do, Korea) within 4 d. Subsequently, a porcelain mortar and pestle were used to grind each sample, and the dry powder was filtered through a mesh sieve. A total of 200 mg dry powder of flowers, leaves, roots, and stems was dissolved in 10 mL of methanol and sonicated for 30 min to determine the concentrations of rosmarinic acid (RA), tilianin, acacetin, and three acacetin glycosides: acacetin 7-*O*-(2″-*O*-acetyl)β-D-glucopyranoside (acacetin 1), acacetin 7-*O*-(6″-*O*-malonyl)β-D-glucopyranoside (acacetin 2), and acacetin 7-*O*-(2″-*O*-acetyl-6″-*O*-malonyl)β-D-glucopyranoside (acacetin 3). The mixed extract was centrifuged at 1358×*g* for 20 min. One mL of the extract solution was passed through a 0.45 μm filter before being analyzed by high-performance liquid chromatography (1260 Infinity, Agilent Technologies, Santa Clara, CA, USA). The mobile phase was composed of 0.1% formic acid in water (solvent A) and acetonitrile (solvent B). The gradient program was as follows: 0–5 min: 20% B, 5–10 min: 50% B, 10–20 min: 50% B, and 20–22 min: 100% B. The injection volume and flow rate were 10 μL and 0.8 mL min^{-1}, respectively. High-performance liquid chromatography (HPLC) analysis was carried out at a temperature of 30 °C using a C18 column (250 mm × 4.6 mm, 5 μm; RS tech, Daejeon, Korea). The HPLC chromatogram was monitored at 330 nm according to An et al., 2018 and Hong et al., 2021 [40,41]. Standard compounds from Sigma−Aldrich (St. Louis, MO, USA) were used to generate the calibration curves. RA, tilianin, and acacetin were detected at 11.655 min, 12.542 min, and 19.659 min, respectively. Acacetins 1, 2, and 3 were detected at 13.131, 14.485, and 15.351 min, respectively [40,41]. The concentrations of RA, tilianin, acacetin, and three acacetin glycosides (bioactive compounds) in the root, leaf, stem, and flower were expressed as per unit dry weight (DW) (mg·g^{-1} DW). The concentration of each bioactive compound in the entire plant (mg·g^{-1} DW) was determined by summing up the product of the amount of each compound present in every plant part and the percentage of dry weight for each plant organ relative to the total dry weight of the entire plant, as indicated in equation (1).

BCx in the entire plant (mg·g^{-1} DW) = Σ (amount of BCx in each part × % dry weight of each plant organ per dry weight of the entire plant).(1)

BC:Concentration of bioactive compound
x: Tilianin, Acacetin a, Acacetin b, Acacetin c, or RA or Acacetin.
The BC content of the entire plant (mg/plant DW) was expressed as the BC concentration (mg·g^{-1} plant DW) multiplied by the entire plant DW (g). For each replicate per $AgNO_3$ treatment, BC concentrations were analyzed using three measurements (n = 3).

2.7. Statistical analysis

For each treatment, growth parameters were collected from five plants (n = 5) and photosynthetic characteristics, photosynthetic pigments, DPPH radical scavenging activity, and bioactive compounds were determined from three plants (n = 3). The experiment was conducted using a completely randomized design and comprised of two replicates. Statistical data were analyzed using SPSS version 20.0 software (SPSS 20, IBM Corp., Armonk, N.Y., USA). The results of the experiment were consolidated and examined using a one-way ANOVA. Tukey's multiple range test was used to compare the means of the treatment groups, and significant differences were

Fig. 2. Images of *A. rugosa* plants growth at different $AgNO_3$ treatments (0-control, 50 μmol mol^{-1}, 100 μmol mol^{-1}, 200 μmol mol^{-1}, and 400 μmol mol^{-1}), subjected to root soaking.

assessed at the 5% level.

The BC concentrations and contents in the plant organs were visualized using a heat map. Rows and columns were grouped using the GraphPad Prism distance and average linkage methods for heatmap construction. The color scale in the heatmap represents numeric differences, with red indicating the largest values, black representing medium values, and green indicating the smallest values for each parameter.

3. Results

3.1. Plant growth parameters

The results evidenced that plant growth significantly declined with increasing concentrations of $AgNO_3$ (Table 1 and Fig. 2). All the measured growth characteristics, that is, the leaf length, leaf area, stem length, shoot and root fresh weights/plant, and root length were significantly decreased at 200 and 400 μmol mol^{-1} of $AgNO_3$ compared to those of the untreated plants. Additionally, the application of 400 μmol mol^{-1} of $AgNO_3$ resulted in a significant decrease in the number of leaves, shoot and root dry weights/plant, and flower and stem dry weights/plant, when compared to those of the untreated plants (Table 1 and Fig. 2). The lowest values of plant growth parameters were found with 400 μmol mol^{-1} of $AgNO_3$ treatment. The stem lengths exhibited a significant reduction of 48.75% compared to those of the untreated plants, as a result of the 400 μmol mol^{-1} $AgNO_3$. The number of leaves and leaf area under 400 μmol mol^{-1} $AgNO_3$ were 20.50% and 46.76%, respectively, being significantly lower than those of the control plants. 400 μmol mol^{-1} treatment significantly decreased the shoot fresh weight and root fresh weight by 51.37% and 45.28%, respectively, compared with those of the untreated plants. The shoot and root dry weights/plant, and flowers and stem dry weights/plant were significantly reduced in the 400 μmol mol^{-1} treatment compared to those of the control plants. These results evidenced that 400 μmol mol^{-1} of $AgNO_3$ strongly reduced the plant growth characteristics of *A. rugosa*.

3.2. Photosynthetic activity

The photosynthetic parameters of *A. rugosa* under different concentrations of $AgNO_3$ stress and the control are illustrated in Fig. 3. The net photosynthetic rate (P_n) and stomatal conductance (g_s) evidenced a decreasing tendency with increased $AgNO_3$ concentrations. When the $AgNO_3$ concentration was raised to 400 μmol mol^{-1}, the P_n and g_s were reduced to the lowest value of 4.71 μmol CO_2

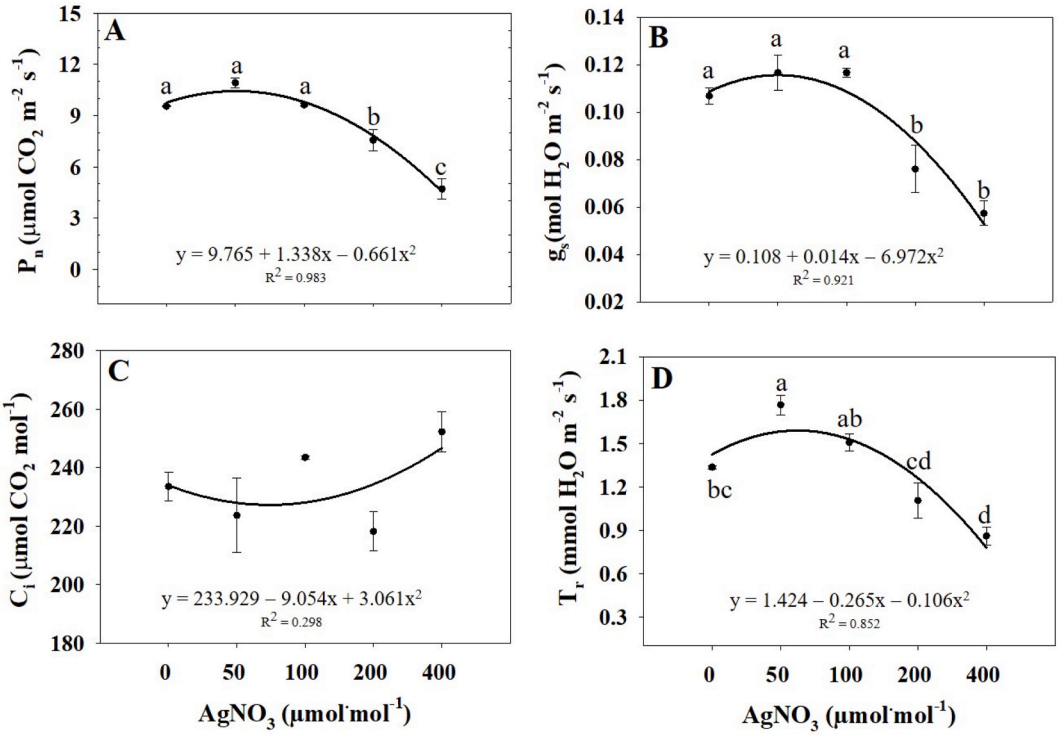

Fig. 3. Net photosynthetic rate (P_n) (**A**), stomatal conductance (g_s) (**B**), intercellular CO_2 concentration (C_i) (**C**), and transpiration rate (T_r) (**D**) of *A. rugosa* at different $AgNO_3$ treatments (0-control, 50 μmol mol^{-1}, 100 μmol mol^{-1}, 200 μmol mol^{-1}, and 400 μmol mol^{-1}). Each value indicates the mean ± SE of three samples (n = 3). Different letters represent significant differences at $p \leq 0.05$, as assessed by ANOVA according to Tukey's multiple range test.

m^{-2} s^{-1} and 0.06 mol H_2O m^{-2} s^{-1}, respectively (Fig. 3A and B). The intercellular CO_2 concentration (C_i) was not significantly different between the $AgNO_3$ treatments and control (Fig. 3C). The transpiration rate (T_r) decreased by 35.65% in the 400 μmol mol^{-1} $AgNO_3$ treated group compared to that of the untreated plants (Fig. 3D). These results indicate that high $AgNO_3$ concentrations strongly influenced the photosynthetic system of *A. rugosa*.

3.3. Photosynthetic pigments and DPPH radical scavenging activity

The chlorophyll *a*, total carotenoid, chlorophyll *a*/b, total chlorophyll, and chlorophyll *b* contents of *A. rugosa* were not significantly different among the control and 0, 50, 100, and 200 μmol mol^{-1} treatments. However, chlorophyll *a*, total carotenoid, chlorophyll *a*/b, total chlorophyll, and chlorophyll *b* were the lowest in the 400 μmol mol^{-1} treatment (Fig. 4A, B, 4C, 4D, and 4E). The DPPH radical scavenging activity was significantly higher in the 50, 100, 200, and 400 μmol mol^{-1} treatments by 20.94%, 19.04%, 16.95%, and 13.33%, respectively, compared to that in the control plants (Fig. 4F). These results demonstrated that the lowest values of chlorophyll and total carotenoid were in the 400 μmol mol^{-1} treatment. However, all $AgNO_3$ treatments increased the DPPH radical-scavenging activity.

3.4. Acacetin, tilianin, and rosmarinic acid concentrations and contents

The concentrations of RA, tilianin, and acacetin differed in diverse organs of *A. rugosa*. The highest concentrations of RA were found in the roots, whereas the highest concentrations of tilianin and acacetin were found in the flowers. The difference in bioactive compound concentrations in each part of *A. rugosa* may be attributed to the movement of bioactive compounds from the root to the shoot. Stems and flowers of *A. rugosa* treated with 400 μmol mol^{-1} $AgNO_3$ accumulated highest amounts of RA (Fig. 5). Roots treated with 50 μmol mol^{-1} $AgNO_3$ exhibited the highest levels of RA concentration. Tilianin concentration was the highest in the treatment group with 100 μmol mol^{-1} $AgNO_3$. The application of $AgNO_3$ did not influence the tilianin concentration in the stems, roots, or leaves compared with that in the untreated plants. Nevertheless, $AgNO_3$ treatment reduced acacetin concentrations in flowers compared to that in untreated plants (Fig. 5).

Due to the reduction in dry weight, higher concentrations of $AgNO_3$ (400 μmol mol^{-1}) resulted in a tendency of decreased RA content in the stems, leaves, and roots in comparison to untreated plants. The lowest tilianin content in flowers was observed under the concentration of 400 μmol mol^{-1}. The tilianin content under 100 μmol mol^{-1} in leaves was higher than those of the other treatments (Fig. 6). $AgNO_3$ treatment reduced acacetin content in flowers and leaves compared to control plants (Fig. 6).

Plants exposed to 400 μmol mol^{-1} had significantly higher RA concentrations (1.10 times) in the entire plant than the untreated plants (Fig. 7A). Treatment with 100 μmol mol^{-1} resulted in significantly higher tilianin concentrations (1.26 times) in the entire plant than that in the untreated plants (Fig. 7B). However, $AgNO_3$ treatment restrained acacetin production in the entire plant compared to that in the untreated plants (Fig. 7C). Furthermore, the RA content was reduced by increasing the dosage of $AgNO_3$ because of the decrease in the dry weight of the entire plant (Fig. 7D). Especially, tilianin contents were greatly increased by 17.88% in the presence

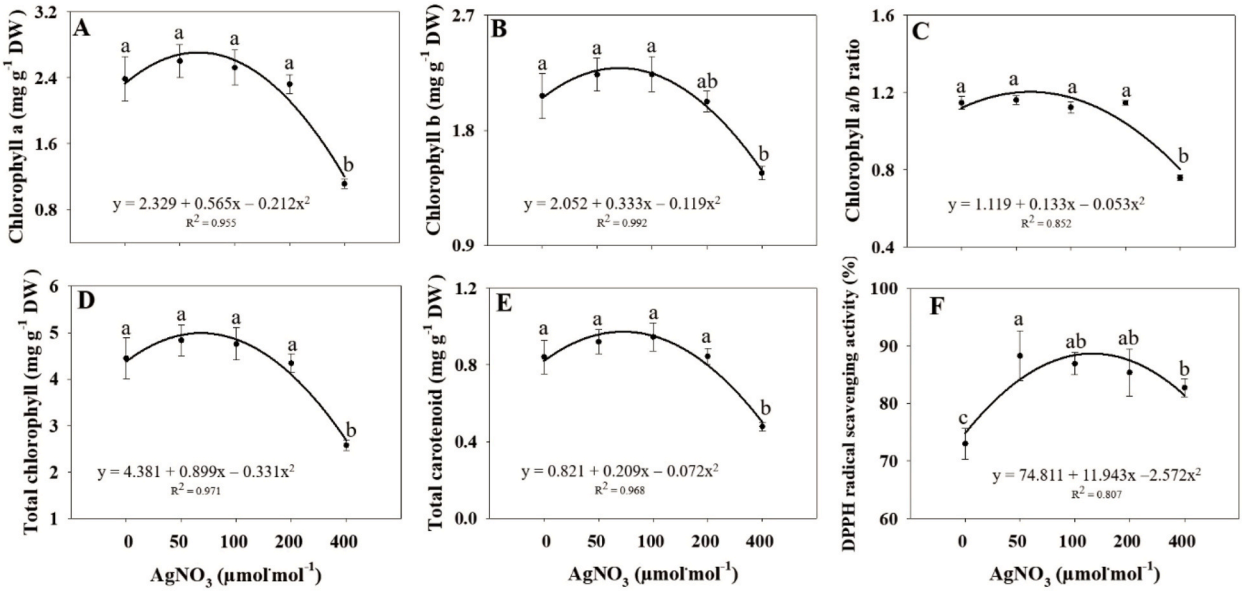

Fig. 4. Chlorophyll *a* (A), chlorophyll *b* (B), chlorophyll *a*/b ratio (C), total chlorophyll (D), total carotenoid (E), and DPPH (F) of *A. rugosa* under different $AgNO_3$ treatments (0-control, 50 μmol mol^{-1}, 100 μmol mol^{-1}, 200 μmol mol^{-1}, and 400 μmol mol^{-1}). Each value indicates the mean ± SE of three samples (n = 3). Different letters represent significant differences at $p \leq 0.05$, as assessed by ANOVA according to Tukey's multiple range test.

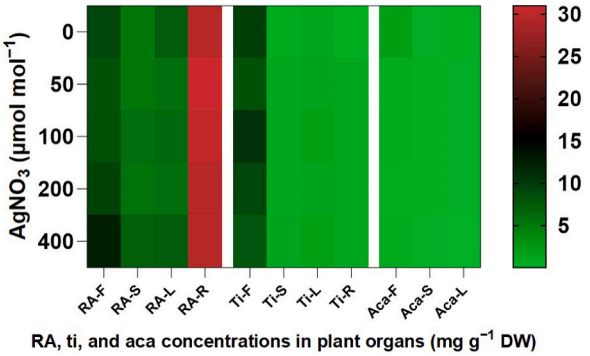

Fig. 5. Heatmap analysis of rosmarinic acid (RA), tilianin (Ti), and acacetin (Aca) concentrations (mg g^{-1} DW) in flowers (F), stems (S), leaves (L), and roots (R) of *A. rugosa* grown at different $AgNO_3$ treatments (0-control, 50 μmol mol^{-1}, 100 μmol mol^{-1}, 200 μmol mol^{-1}, and 400 μmol mol^{-1}). The color scale in the heatmap represents numeric differences, with red indicating the largest values, black representing medium values, and green indicating the smallest values for each parameter, respectively. $AgNO_3$ treatments are grouped in the rows; RA, Ti, and Aca concentrations in each plant organ are grouped in the columns.

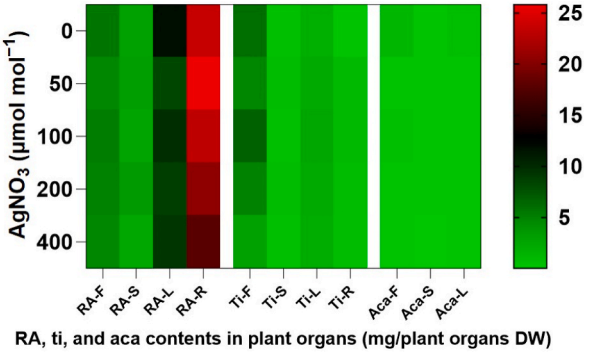

Fig. 6. Heatmap analysis of rosmarinic acid (RA), tilianin (Ti), and acacetin (Aca) contents (mg/plant organs DW) in flowers (F), stems (S), leaves (L), and roots (R) of *A. rugosa* grown at different $AgNO_3$ treatments (0-control, 50 μmol mol^{-1}, 100 μmol mol^{-1}, 200 μmol mol^{-1}, and 400 μmol mol^{-1}). The color scale in the heatmap represents numeric differences, with red indicating the largest values, black representing medium values, and green indicating the smallest values for each parameter, respectively. $AgNO_3$ treatments are grouped in the rows; RA, Ti, and Aca concentrations in each plant organ are grouped in the columns.

of 100 μmol mol^{-1}, compared to that in the control plants (Fig. 7E). In contrast, increasing the dosage of $AgNO_3$ led to a progressive reduction in acacetin content due to the low dry weight of the whole plant. Further details reveal that the application of treatment with a concentration of 400 μmol mol^{-1} resulted in the maximal reduction of acacetin contents accumulated in the whole plant, exhibiting an impressive reduction of 77.37% compared to that of the untreated plants (Fig. 7F).

3.5. Acacetin 7-O-(2″-O-acetyl)β-D-glucopyranoside (acacetin 1), acacetin 7-O-(6″-O-malonyl)β-D-glucopyranoside (acacetin 2), and acacetin 7-O-(2″-O-acetyl-6″-malonyl)β-D-glucopyranoside (acacetin 3) concentrations and contents

Concentration of acacetin 1 in the leaves with 100 μmol mol^{-1} was highest value (Fig. 8). Application of $AgNO_3$ at 50, 200 and 400 μmol mol^{-1} indicated higher values of acacetin 2 concentration in the flowers compared with that in the untreated plants. Concentration of acacetin 2 in the stems and leaves under treatment with $AgNO_3$ was increased compared with that in the untreated plants. The concentration of acacetin 3 in the flowers was higher under 50 and 200 μmol mol^{-1} among the $AgNO_3$ treatments and the control group, whereas in the stems, under treatment with $AgNO_3$, it was increased compared with that in the untreated plants. The most notable concentrations of acacetin 3 were discovered in the leaves under 200 μmol mol^{-1}, demonstrating the highest values (Fig. 8).

Application of 400 μmol mol^{-1} $AgNO_3$ reduced acacetin 1 contents in the flowers (Fig. 9). Treatment with 50 and 200 μmol mol^{-1} $AgNO_3$ resulted in higher acacetin 1 content in the stems compared to that in the untreated plants (Fig. 9). The acacetin 1 content in the leaves was decreased in response to treatments with 50 and 400 μmol mol^{-1} $AgNO_3$, when compared to that in the untreated plants. The application of 400 μmol mol^{-1} $AgNO_3$ treatments decreased the acacetin 2 contents in flowers when compared to that in the untreated plants. The treatments with 100 and 200 μmol mol^{-1} $AgNO_3$ led to elevated acacetin 2 contents in leaves, surpassing those observed in the control plants. In contrast, the application of 400 μmol mol^{-1} $AgNO_3$ resulted in the lowest acacetin 3 content in flowers compared to that in the other treatments. The application of 50 and 200 μmol mol^{-1} $AgNO_3$ treatments enhanced the acacetin

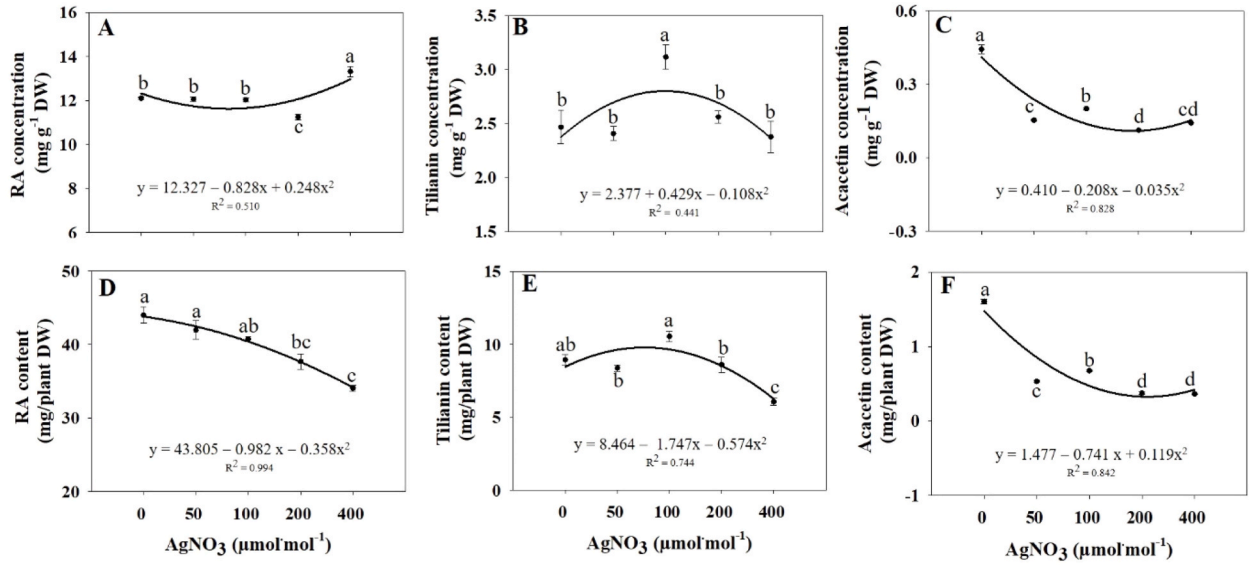

Fig. 7. Rosmarinic acid (RA) concentration (A) and content (D), tilianin concentration (B) and content (E), acacetin concentration (C) and content (F) in whole plant of *A. rugosa* at different $AgNO_3$ treatments (0-control, 50 μmol mol^{-1}, 100 μmol mol^{-1}, 200 μmol mol^{-1}, and 400 μmol mol^{-1}). Each value indicates the mean ± SE of three samples (n = 3). Different letters represent significant differences at $p \leq 0.05$, as assessed by ANOVA according to Tukey's multiple range test.

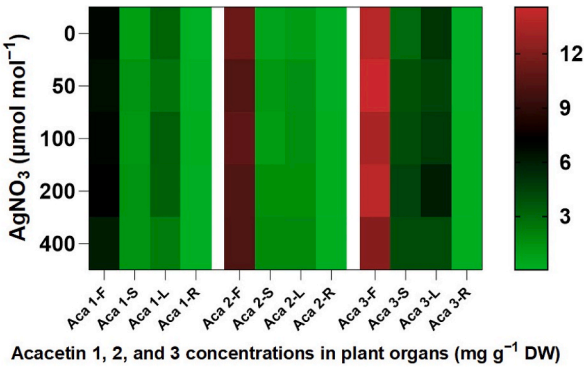

Fig. 8. Heatmap analysis of acacetin 7-*O*-(2″-*O*-acetyl)β-D-glucopyranoside (**Aca 1**), acacetin 7-*O*-(6″-*O*-malonyl)β-D-glucopyranoside (**Aca 2**), and acacetin 7-*O*-(2″-*O*-acetyl-6″-malonyl)β-D-glucopyranoside **(Aca 3)** concentrations (mg g^{-1} DW) in flowers (F), stems (S), leaves (L), and roots (R) of *A. rugosa* grown at different $AgNO_3$ treatments (0-control, 50 μmol mol^{-1}, 100 μmol mol^{-1}, 200 μmol mol^{-1}, and 400 μmol mol^{-1}). The color scale in the heatmap represents numeric differences, with red indicating the largest values, black representing medium values, and green indicating the smallest values for each parameter, respectively. $AgNO_3$ treatments are grouped in the rows; RA, Ti, and Aca concentrations in each plant organ are grouped in the columns.

3 content in stems compared to that in untreated plants. Among the various treatments, the acacetin 3 content in leaves reached its highest value under the application of 200 μmol mol^{-1} (Fig. 9).

A slight increase in acacetin 1 concentration was recorded in the 100 and 200 μmol mol^{-1} treatments (8.99% and 5.31%, respectively) compared to that in the untreated plants (Fig. 10A). The plants treated with 100 μmol mol^{-1} exhibited significantly increased acacetin 2 concentration by 12.78%, compared to that in the untreated plants (Fig. 10B). The application of 200 μmol mol^{-1} resulted in a significant increase of 11.90% in the concentration of acacetin 3 compared to that in the untreated plants (Fig. 10C). These results demonstrated that $AgNO_3$ positively affects the accumulation of bioactive compounds in *A. rugosa*. In contrast, 50 and 400 μmol mol^{-1} treatments significantly decreased the acacetin 1 content by 15.47% and 44.15%, respectively, compared with that in the control, from the reduction in the dry weight of the entire plant (Fig. 10D). However, a significant reduction in acacetin 2 and acacetin 3 contents was only recorded under the 400 μmol mol^{-1} treatment. The mean acacetin 2 and 3 contents decreased by 27.87% and 40.25% in the 400 μmol mol^{-1} treatment, respectively, compared to that in the untreated plants (Fig. 10E and F).

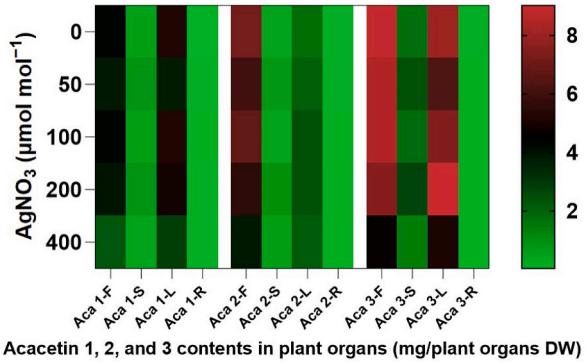

Fig. 9. Heatmap analysis of acacetin 7-*O*-(2″-*O*-acetyl)β-D-glucopyranoside (**Aca 1**), acacetin 7-*O*-(6″-*O*-malonyl)β-D-glucopyranoside (**Aca 2**), and acacetin 7-*O*-(2″-*O*-acetyl-6″-malonyl)β-D-glucopyranoside **(Aca 3)** contents (mg/plant organs DW) in flowers (F), stems (S), leaves (L), and roots (R) of *A. rugosa* grown at different $AgNO_3$ treatments (0-control, 50 μmol mol^{-1}, 100 μmol mol^{-1}, 200 μmol mol^{-1}, and 400 μmol mol^{-1}). The color scale in the heatmap represents numeric differences, with red indicating the largest values, black representing medium values, and green indicating the smallest values for each parameter, respectively. $AgNO_3$ treatments are grouped in the rows; RA, Ti, and Aca concentrations in each plant organ are grouped in the columns.

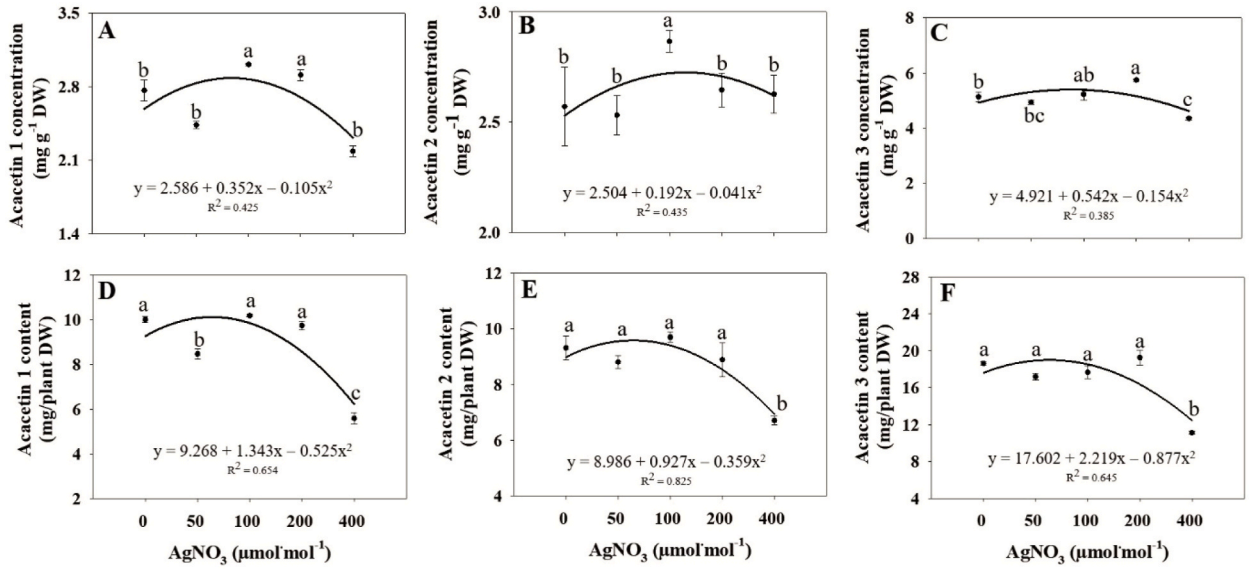

Fig. 10. Acacetin 7-*O*-(2″-*O*-acetyl)β-D-glucopyranoside (Acacetin 1) (A and D), Acacetin 7-*O*-(6″-*O*-malonyl)β-D-glucopyranoside (Acacetin 2) (B and E), and Acacetin 7-*O*-(2″-*O*-acetyl-6″-malonyl)β-D-glucopyranoside (Acacetin 3) (C and F), concentrations and contents in whole plant of *A. rugosa* at different $AgNO_3$ treatments (0-control, 50 μmol mol^{-1}, 100 μmol mol^{-1}, 200 μmol mol^{-1}, and 400 μmol mol^{-1}). Each value indicates the mean ± SE of three samples (n = 3). Different letters represent significant differences at $p \leq 0.05$, as assessed by ANOVA according to Tukey's multiple range test.

4. Discussion

4.1. Plant growth parameters

Any abiotic stress reduces growth [42], and causes various physiological changes in plants, including the creation of osmotic stress [43], ROS, oxidative stress [44], reduction of photosynthetic activity [45], and macro-and micronutrients imbalance, including [46]. It also triggers biochemical changes in enzymatic antioxidants such as superoxide dismutase (SOD), catalase (CAT), and glutathione peroxidase (GPX) [47], and non-enzymatic antioxidants such as phenols [48], hydroxybenzoic acids [10], flavanols [12], beta-carotene [49], flavanones [50], xanthophylls [51], hydroxycinnamic acids [52], flavonols [53], flavones [54], ascorbic acids [55], antiradical capacity [56], and carotenoids [57]. This study was conducted to determine the optimal $AgNO_3$ concentration for diniconazole base in *A. rugosa* plants. Diniconazole decreased almost all plant growth parameters of *A. rugosa*, except for root length, compared with those in the control plants [22]. Diniconazole, a growth regulator belonging to the triazole family, restricts elongation

of stems [58]. Diniconazole, an N-containing heterocyclic compound, inhibits cytochrome of oxidative demethylation mediated by cytochrome P450. This is closely associated with the conversion of kaurene to kaurenoic acid, which plays a role in the biosynthesis of gibberellin [59]. By inducing stem elongation, diniconazole curbs gibberellin activity within the plant cells, resulting in reduced stem length [60]. Diniconazole is a useful tool for decreasing the height of *A. rugosa* plants, allowing for the expansion of cultivation layers in plant factories [22]. Exposure to high $AgNO_3$ concentrations significantly reduced plant growth characteristics in *A. rugosa*, which may be directly related to decreased photosynthetic performance. A significant decrease in stem length, leaf area, leaf length, the fresh weights of shoot and root, and root length under 200 and 400 μmol mol^{-1} treatments was observed compared to those in the control treatment (Table 1, Figs. 1, and Fig. 2). A similar result was found by Krishnaraj et al., 2012 [32] who reported that using $AgNO_3$ did not lead to intense toxic effects on morphology, as observed on scanning electron microscopy. Plant growth is restricted at high $AgNO_3$ concentrations (Krishnaraj et al., 2012). The fresh weight, shoot and root lengths, and photosynthetic characteristics of *Brassica* sp. under $AgNO_3$ treatment were lower than those of the untreated plants. Moreover, $AgNO_3$ accumulation in the roots was greater than that in other organs of *Brassica* sp. plants [23]. Tobacco root growth was significantly promoted at lower silver nanoparticle (AgNP) concentrations of 25 and 50 μM and significantly decreased after exposure to higher concentrations of 75, 100, and 150 μM [61]. Seedling growth in *Brassica napus* L. was restricted by $AgNO_3$ [62]. The growth characteristics of live plants are reduced by high $AgNO_3$ concentrations because of the increased absorption of silver [63]. Corn root elongation is negatively affected by AgNP toxicity [64]. The association between silver ions (Ag^+) and sunflower plant roots distorts the epidermal structure and changes its anatomical properties. Therefore, root hairs are damaged [65]. The high silver accumulation in plants associated with the root and the translocation element ([Ag]shoot/[Ag]root) was relatively low, and a high dose of Ag (40 mg L^{-1}) reduced leaf growth of wetland plants up to 55% [66]. In this study, plant growth of *A. rugosa* was reduced by higher $AgNO_3$ concentrations (200 and 400 μmol mol^{-1}), which may be due to the absorption of $AgNO_3$ through the roots, changes in the cell and membrane structures, defensive mechanisms, high $AgNO_3$ accumulation in plants, and $AgNO_3$ toxicity.

4.2. Photosynthetic parameters, photosynthetic pigment, and DPPH radical scavenging activity

The net photosynthetic rate was decreased with higher $AgNO_3$ exposure (200 and 400 μmol mol^{-1}) (Fig. 3). The results of this study are consistent with those of previous studies, which indicate that high concentrations of AgNPs and $AgNO_3$ inhibit photosynthetic parameters in several plant species, such as *Chlamydomonas reinhardtii* [67], aquatic plants [68], *Brassica* sp. [23], pearl millet [34], and tobacco seedlings [61]. Photosynthetic parameters of this study were lower under higher $AgNO_3$ concentrations (200 and 400 μmol mol^{-1}) than those in the control plants because of the toxicity influence of $AgNO_3$. A similar study conducted by Khan et al., 2019 [34] found that photosynthetic parameters were lower in AgNP-treated plants than those in untreated plants. A reduction in photosynthesis and plant growth may be the result of the destructive effects of ROS on the photosynthetic machinery and might be related to oxidative stress [33]. $AgNO_3$ caused a significant decrease in photosystem II activity, which finally reduced the photosynthetic parameter values and decreased the plant chlorophyll content [34]. This decrease in photosynthesis under high $AgNO_3$ concentrations may be attributed to ROS-mediated damage to biomolecules related to the photosynthetic system, which is predominantly related to the membranes of the energy transaction system.

Photosynthetic ability can be explored by determining the chlorophyll parameters under $AgNO_3$ stress and normal conditions [23]. The results verified that under 400 μmol mol^{-1} exposure, the chlorophyll *a*, total carotenoid, chlorophyll *a*/b, total chlorophyll, and chlorophyll *b* contents of *A. rugosa* were reduced (Fig. 4). The substantial reduction in chlorophyll and total carotenoid content indicated modifications in the function and structure of the photosynthetic process. This may be related to decreased biomass accumulation in *A. rugosa*. Heavy metals can alter physiological processes, particularly by reducing the synthesis of photosynthetic pigments [69,70]. This may indicate that Ag^+ caused a water imbalance. Therefore, plant photosynthesis is restricted to the highest concentration of $AgNO_3$. The decrease in chlorophyll content under high $AgNO_3$ concentrations may be ascribed to ROS-mediated damage to the biomolecules connected to the photosynthetic system, which is predominantly related to the membranes of the energy transaction system [71]. $AgNO_3$ treatment increased DPPH free radical scavenging activity (Fig. 4F). ROS are generated because $AgNO_3$ stress damages macromolecules and ultimately cellular structure in plants [72]. Abiotic stress causes oxidative damage in a considerable proportion of plants. However, free radical scavenging and antioxidant system capacities are also controlled [73]. AgNPs and $AgNO_3$ significantly increased the DPPH free radical scavenging activity of *Echium amoenum* [74]. In line with these results, AgNPs demonstrated to enhance DPPH radical scavenging activity in *Erythrina suberosa* [75]. The data of this study also evidenced that $AgNO_3$ increased the DPPH scavenging activity (Fig. 4F).

4.3. Acacetin, tilianin, rosmarinic acid, and three acacetin glycoside concentrations and contents

The concentration of RA in the entire plant of *A. rugosa* was higher than that of tilianin and acacetin (Fig. 7). A similar finding was reported by Tuan et al., 2012 [76], who observed that the concentration of RA in *A. rugosa* was higher than that of tilianin and acacetin. Furthermore, RA is an important phenolic compound, with its primary concentration observed in the hairy roots of *A. rugosa* [77]. Our findings are consistent with this observation as we detected the highest concentration of RA in the roots of *A. rugosa* compared to that in other plant organs (Fig. 5). Similarly, the roots of *A. rugosa* exhibited the highest concentration of RA compared to that in other organs [78]. This distribution pattern can be attributed to the movement of bioactive compounds from the roots to other parts of the plant, influencing their concentrations in different organs. The effects of $AgNO_3$ treatment on the accumulation of these bioactive compounds were also investigated. The stems and flowers treated with 400 μmol mol^{-1} $AgNO_3$ exhibited the highest accumulation of RA. This suggests that the application of $AgNO_3$ at this concentration enhanced RA production in these plant parts. In the case of

tilianin, $AgNO_3$ treatment with 100 μmol mol^{-1} increase its concentration in the flower compared to that in the other plants. This indicates that $AgNO_3$ application may have a positive effect on tilianin accumulation in flowers. Conversely, $AgNO_3$ treatment led to a reduction in acacetin concentration in flowers. This study provides valuable insights into the differential accumulation of RA, tilianin, and acacetin in different organs of *A. rugosa* and the influence of $AgNO_3$ treatment on their concentrations. These findings highlight the potential use of $AgNO_3$ to enhance the production of bioactive compounds in specific plant parts, which may have implications for their use in various applications.

$AgNO_3$ causes considerable phytotoxicity in plants, which can be observed by analyzing various physiological, physical, structural, and biochemical traits [23]. $AgNO_3$ has been reported to be effective in promoting RA in *A. rugosa* [79]. Similarly, the RA concentrations of *A. rugosa* were significantly higher with exposure to high $AgNO_3$ concentrations (400 μmol mol^{-1}) (Fig. 7A). Among the different treatments, the highest value of tilianin concentration and content was achieved at 100 μmol mol^{-1} (Fig. 7B and E). The results depicted in Fig. 10A demonstrate that the concentrations of acacetin 1 were notably higher in the plants treated with 100 and 200 μmol mol^{-1} compared to those in the untreated plants. Fig. 10B reveals a significant elevation in the concentration of acacetin 2 in the plants treated with 100 μmol mol^{-1} when compared to that in the untreated plants. Additionally, Fig. 10C displays that the application of 200 μmol mol^{-1} resulted in the highest concentration of acacetin 3 among treatments. The individual phenolic compounds, flavonoid content, and total phenolic content in *Cucumis anguria* were increased by the AgNPs [80]. Malondialdehyde, hydrogen peroxide, glucosinolates, and phenolic compounds were significantly enhanced by AgNPs [81]. Superoxide dismutase, peroxidase, guaiacol peroxidase, total phenolics, glutathione reductase activity, ascorbate peroxidase, total flavonoid content, proline content, and catalase activity in pearl millet were increased by $AgNO_3$ [34]. Ag^+ released from $AgNO_3$ are severely toxic to plants [82]. Ag^+ stress stimulates ROS production and promotes oxidative damage. Therefore, plants have created an antioxidant defense system to deal with oxidative stress in cells [68]. Ag^+ enhance ROS production and restrict enzymatic antioxidants. $AgNO_3$ stress in plants leads to increased ROS production, which affects plant metabolism by destroying defense mechanisms and reducing antioxidant activities [83]. ROS are produced in cells because of Ag^+ toxicity [84]. $AgNO_3$ damages cell membranes and interrupts DNA replication and ATP production [82]. The subsequent generation of oxidative stress and ROS production results in different toxic effects and may affect gene expression and DNA degradation [85]. Total proline and phenolic contents in *Solanum tuberosum* were considerably increased by $AgNO_3$ and AgNP treatments compared to those in the untreated plants [36]. The accumulation of indole and phenolic compounds, including hydroxycamalexin malonyl-hexoside, camalexin, and hydroxycamalexin O-hexoside in *Arabidopsis thaliana* was increased by Ag^+ and silver nanoparticle treatments [86]. In line with previous results, in this study RA, tilianin, and concentration of acacetin 1, 2, and 3 in *A. rugosa* significantly increased at various $AgNO_3$ concentrations.

5. Conclusion

These results demonstrate that $AgNO_3$ improved the bioactive compounds in *A. rugosa* under hydroponic culture conditions in a plant factory. The treatments with 200 and 400 μmol mol^{-1} $AgNO_3$ led to a significant decrease in plant growth parameters compared to those of other treatments. However, 400 μmol mol^{-1} exhibited an elevated concentration of RA in the whole plant, while the highest tilianin concentration and content were observed in the 100 μmol mol^{-1} treatment. Concentration of acacetin 1 in the whole plant significantly increased under 100 and 200 μmol mol^{-1} treatments compared to that in the untreated plants, while concentrations of acacetin 2 and 3 were the highest in the 100 and 200 μmol mol^{-1} treatments, respectively. This study suggests that the 100 μmol mol^{-1} treatment of $AgNO_3$ can be utilized to enhance the bioactive compound content in *A. rugosa* without severely impeding plant growth or significantly reducing chlorophyll concentrations. This optimal dose may provide a practical and effective approach for growers and researchers to cultivate *A. rugosa* and harness its health benefits. Given that we soaked selected concentrations of $AgNO_3$ for 10 min in this study, further studies are required to explore the optimal soaking duration for $AgNO_3$ from an application perspective.

Author contribution statement

Vu Phong Lam and Jongseok Park: Conceived and designed the experiments; Performed the experiments; Contributed reagents, materials, analysis tools or data; Wrote the paper.

Lee Beomseon: Performed the experiments; Wrote the paper.

Vu Ky Anh: Conceived and designed the experiments; Performed the experiments; Contributed reagents, materials, analysis tools or data.

Dao Nhan Loi: Conceived and designed the experiments; Performed the experiments; Contributed reagents, materials, analysis tools or data.

Sunwoo Kim and Lee Kwang-ya: Analysis tools or data; Wrote the paper.

Data availability statement

Data included in article/supp. material/referenced in article.

Declaration of competing interest

The authors declare that they have no known competing financial interests or personal relationships that could have appeared to influence the work reported in this paper.

Acknowledgments

This work was supported by Korea Institute of Planning and Evaluation for Technology in Food, Agriculture and Forestry (IPET) and Korea Smart Farm R&D Foundation (KosFarm) through Smart Farm Innovation Technology Development Program, funded by Ministry of Agriculture, Food and Rural Affairs (MAFRA) and Ministry of Science and ICT (MSIT), Rural Development Administration (RDA) (421034–04).

Appendix A. Supplementary data

Supplementary data to this article can be found online at https://doi.org/10.1016/j.heliyon.2023.e20205.

References

[1] L.Y. Sim, N.Z. Abd Rani, K. Husain, Lamiaceae: an insight on their anti-allergic potential and its mechanisms of action, Front. Pharmacol. 10 (2019) 667, https://doi.org/10.3389/fphar.2019.00677.
[2] S. Zielinska, A. Matkowski, Phytochemistry and bioactivity of aromatic and medicinal plants from the genus *Agastache* (Lamiaceae), Phytochemistry Rev. 13 (2014) 391–416, https://doi.org/10.1007/s11101-014-9349-1.
[3] H.J. Yeo, C.H. Park, Y.E. Park, H. Hyeon, J.K. Kim, S.Y. Lee, S.U. Park, Metabolic profiling and antioxidant activity during flower development in *Agastache rugosa*, Physiol. Mol. Biol. Plants 27 (2021) 445–455, https://doi.org/10.1007/s12298-021-00945-z.
[4] H.Y. Gong, L.J. He, S.Y. Li, C. Zhang, M.A. Ashraf, Antimicrobial, antibiofilm and antitumor activities of essential oil of *Agastache rugosa* from Xinjiang, China, Saudi J. Biol. Sci. 23 (2016) 524–530, https://doi.org/10.1016/j.sjbs.2016.02.020.
[5] A. Lashkari, F. Najafi, G. Kavoosi, S. Niazi, Evaluating the *In vitro* anti-cancer potential of estragole from the essential oil of *Agastache foeniculum* [Pursh.] Kuntze, Biocatal. Agric. Biotechnol. 27 (2020), https://doi.org/10.1016/j.bcab.2020.101727.
[6] H.H. Nam, et al., Pharmacological effects of *Agastache rugosa* against gastritis using a network pharmacology approach, Biomolecules 10 (2020), https://doi.org/10.3390/biom10091298.
[7] H.Y. Gong, S.Y. Li, L.J. He, R. Kasimu, Microscopic identification and in vitro activity of *Agastache rugosa* (Fisch et Mey) from Xinjiang, China, Bmc Complem Altern M 17 (2017), https://doi.org/10.1186/s12906-017-1605-7.
[8] P. Cao, P.Y. Xie, X.B. Wang, J.M. Wang, J.F. Wei, W.Y. Kang, Chemical constituents and coagulation activity of *Agastache rugosa*, Bmc Complem Altern M 17 (2017), https://doi.org/10.1186/s12906-017-1592-8.
[9] Y. Oh, H.W. Lim, Y.H. Huang, H.S. Kwon, C.D. Jin, K. Kim, C.J. Lim, Attenuating properties of *Agastache rugosa* leaf extract against ultraviolet-B-induced photoaging via up-regulating glutathione and superoxide dismutase in a human keratinocyte cell line, J. Photochem. Photobiol., B 163 (2016) 170–176, https://doi.org/10.1016/j.jphotobiol.2016.08.026.
[10] U. Sarker, S. Ercisli, Salt eustress induction in red amaranth (*Amaranthus gangeticus*) augments nutritional, phenolic acids and antiradical potential of leaves, Antioxidants 11 (2022), https://doi.org/10.3390/antiox11122434.
[11] U. Sarker, S. Oba, Phenolic profiles and antioxidant activities in selected drought-tolerant leafy vegetable amaranth, Sci. Rep. 10 (2020), https://doi.org/10.1038/s41598-020-71727-y.
[12] U. Sarker, M.N. Hossain, S. Oba, S. Ercisli, R.A. Marc, K.S. Golokhvast, Salinity stress ameliorates pigments, minerals, polyphenolic profiles, and antiradical capacity in lalshak, Antioxidants 12 (2023), https://doi.org/10.3390/antiox12010173.
[13] U. Sarker, M.N. Hossain, M.A. Iqbal, S. Oba, Bioactive components and radical scavenging activity in selected advance lines of salt-tolerant vegetable amaranth, Front. Nutr. 7 (2020), https://doi.org/10.3389/fnut.2020.587257.
[14] U. Sarker, S. Oba, Polyphenol and flavonoid profiles and radical scavenging activity in leafy vegetable *Amaranthus gangeticus*, BMC Plant Biol. 20 (2020), https://doi.org/10.1186/s12870-020-02700-0.
[15] U. Sarker, S. Oba, Nutraceuticals, phytochemicals, and radical quenching ability of selected drought-tolerant advance lines of vegetable amaranth, BMC Plant Biol. 20 (2020), https://doi.org/10.1186/s12870-020-02780-y.
[16] A.K. Jang, et al., Metabolites identification for major active components of *Agastache rugosa* in rat by UPLC-Orbitap-MS: comparison of the difference between metabolism as a single component and as a component in a multi-component extract, J Pharmaceut Biomed (2022) 220, https://doi.org/10.1016/j.jpba.2022.114976.
[17] S. Singh, P. Gupta, A. Meena, S. Luqman, Acacetin, a flavone with diverse therapeutic potential in cancer, inflammation, infections and other metabolic disorders, Food Chem. Toxicol. 145 (2020), https://doi.org/10.1016/j.fct.2020.111708.
[18] M.R. Akanda, M.N. Uddin, I.S. Kim, D. Ahn, H.J. Tae, B.Y. Park, The biological and pharmacological roles of polyphenol flavonoid tilianin, Eur. J. Pharmacol. 842 (2019) 291–297, https://doi.org/10.1016/j.ejphar.2018.10.044.
[19] C.X. Luo, et al., A Review of the anti-inflammatory effects of rosmarinic acid on inflammatory diseases, Front. Pharmacol. 11 (2020), https://doi.org/10.3389/fphar.2020.00153.
[20] L. Graamans, E. Baeza, A. van den Dobbelsteen, I. Tsafaras, C. Stanghellini, Plant factories versus greenhouses: comparison of resource use efficiency, Agric. Syst. 160 (2018) 31–43, https://doi.org/10.1016/j.agsy.2017.11.003.
[21] M.-J. Jung, H.-Y. Kim, K.-B. Lim, Effect of diniconazole on the growth and taking roots after transplanting of *Sesamum indicum* 'Baekseol' plug seedlings, J. Crop Sci. Biotechnol 23 (2020) 235–239, https://doi.org/10.1007/s12892-020-00029-6.
[22] V.P. Lam, V.K. Anh, D.N. Loi, J. Park, Minimizing plant height and optimizing bioactive compound accumulation of *Agastache rugosa* (Fisch. & C.A.Mey.) kuntze by spraying or soaking with diniconazole in a plant factory, Plant Growth Regul. (2023), https://doi.org/10.1007/s10725-023-00974-6.
[23] K. Vishwakarma, et al., Differential phytotoxic impact of plant mediated silver nanoparticles ($AgNP_s$) and silver nitrate ($AgNO_3$) on *Brassica* sp, Front. Plant Sci. 8 (2017), https://doi.org/10.3389/fpls.2017.01501.
[24] C. Vannini, G. Domingo, E. Onelli, B. Prinsi, M. Marsoni, L. Espen, M. Bracale, Morphological and proteomic responses of *Eruca sativa* exposed to silver nanoparticles or silver nitrate, PLoS One 8 (2013), https://doi.org/10.1371/journal.pone.0068752.
[25] C.L. Hyde, G.C. Phillips, Silver nitrate promotes shoot development and plant regeneration of Chile pepper (*Capsicum annuum* L) via organogenesis, In Vitro Cell Dev-Pl 32 (1996) 72–80, https://doi.org/10.1007/BF02823134.
[26] F. Nejatzadeh-Barandozi, F. Darvishzadeh, A. Aminkhani, Effect of nano silver and silver nitrate on seed yield of (*Ocimum basilicum* L.), Org Med Chem Lett 4 (2014) 11, https://doi.org/10.1186/s13588-014-0011-0.
[27] S.S. Gao, I.S. Zhao, S. Duffin, D. Duangthip, E.C.M. Lo, C.H. Chu, Revitalising silver nitrate for caries management, Int. J. Environ. Res. Publ. Health 15 (2018), https://doi.org/10.3390/ijerph15010080.
[28] J. Boenigk, et al., Effects of silver nitrate and silver nanoparticles on a planktonic community: general trends after short-term exposure, PLoS One 9 (2014), https://doi.org/10.1371/journal.pone.0095340.
[29] M. Ejaz, N.I. Raja, Z.U.R. Mashwani, M.S. Ahmad, M. Hussain, M. Iqbal, Effect of silver nanoparticles and silver nitrate on growth of rice under biotic stress, IET Nanobiotechnol. 12 (2018) 927–932, https://doi.org/10.1049/iet-nbt.2018.0057.

[30] D. Karakaya, H. Padem, The effects of silver nitrate applications on the flower quantity of cucumbers (*Cucumis sativus* L.), Not Bot Horti Agrobo 39 (2011) 139–143, https://doi.org/10.15835/nbha3914640.

[31] W.M.R.M. Adly, Y.S.A. Mazrou, M.E. EL-Denary, M.A. Mohamed, E.T. Abd El-Salam, A.S. Fouad, Boosting polyamines to enhance shoot regeneration in potato (*Solanum tuberosum* L.) using $AgNO_3$, Horticulturae 8 (2022), https://doi.org/10.3390/horticulturae8020113.

[32] C. Krishnaraj, E.G. Jagan, R. Ramachandran, S.M. Abirami, N. Mohan, P.T. Kalaichelvan, Effect of biologically synthesized silver nanoparticles on *Bacopa monnieri* (Linn.) Wettst. plant growth metabolism, Process Biochem 47 (2012) 651–658, https://doi.org/10.1016/j.procbio.2012.01.006.

[33] A. Tripathi, S. Liu, P.K. Singh, N. Kumar, A.C. Pandey, D.K. Tripathi, D.K. Chauhan, S.J.P.G. Sahi, Differential phytotoxic responses of silver nitrate ($AgNO_3$) and silver nanoparticle (AgNps) in *Cucumis sativus* L, Plant Gene 11 (2017) 255–264, https://doi.org/10.1016/j.plgene.2017.07.005.

[34] I. Khan, et al., Physiological and biochemical responses of pearl millet (*Pennisetum glaucum* L.) seedlings exposed to silver nitrate ($AgNO_3$) and silver nanoparticles (AgNPs), Int. J. Environ. Res. Publ. Health 16 (2019), https://doi.org/10.3390/ijerph16132261.

[35] H.F. Qian, X.F. Peng, X. Han, J. Ren, L.W. Sun, Z.W. Fu, Comparison of the toxicity of silver nanoparticles and silver ions on the growth of terrestrial plant model *Arabidopsis thaliana*, J Environ Sci 25 (2013) 1947–1955, https://doi.org/10.1016/S1001-0742(12)60301-5.

[36] M.B. Homaee, A.A. Ehsanpour, Physiological and biochemical responses of potato (*Solanum tuberosum*) to silver nanoparticles and silver nitrate treatments under in vitro conditions, Indian J. Plant Physiol. 20 (2015) 353–359, https://doi.org/10.1007/s40502-015-0188-x.

[37] H.K. Lichtenthaler, Chlorophylls and carotenoids - pigments of photosynthetic biomembranes, Method Enzymol 148 (1987) 350–382, https://doi.org/10.1016/0076-6879(87)48036-1.

[38] R.M.A. Machado, I. Alves-Pereira, D. Lourenco, R.M.A. Ferreira, Effect of organic compost and inorganic nitrogen fertigation on spinach growth, phytochemical accumulation and antioxidant activity, Heliyon 6 (2020), https://doi.org/10.1016/j.heliyon.2020.e05085.

[39] M.M. Rahman, M.B. Islam, M. Biswas, A.H. Khurshid Alam, In vitro antioxidant and free radical scavenging activity of different parts of *Tabebuia pallida* growing in Bangladesh, BMC Res. Notes 8 (2015) 621, https://doi.org/10.1186/s13104-015-1618-6.

[40] S. Hong, K.H. Cha, D.Y. Kwon, Y.J. Son, S.M. Kim, J.H. Choi, G. Yoo, C.W. Nho, *Agastache rugosa* ethanol extract suppresses bone loss via induction of osteoblast differentiation with alteration of gut microbiota, Phytomedicine 84 (2021), https://doi.org/10.1016/j.phymed.2021.153517.

[41] J.H. An, H.J. Yuk, D.-Y. Kim, C.W. Nho, D. Lee, H.W. Ryu, S.-R. Oh, Evaluation of phytochemicals in *Agastache rugosa* (Fisch. & C.A.Mey.) Kuntze at different growth stages by UPLC-QTof-MS, Ind. Crops Prod. 112 (2018) 608–616, https://doi.org/10.1016/j.indcrop.2017.12.050.

[42] U. Sarker, S. Oba, Salinity stress enhances color parameters, bioactive leaf pigments, vitamins, polyphenols, flavonoids and antioxidant activity in selected Amaranthus leafy vegetables, J Sci Food Agr 99 (2019) 2275–2284, https://doi.org/10.1002/jsfa.9423.

[43] U. Sarker, S. Oba, The response of salinity stress-induced a. Tricolor to growth, anatomy, physiology, non-enzymatic and enzymatic antioxidants, Front. Plant Sci. 11 (2020), https://doi.org/10.3389/fpls.2020.559876.

[44] U. Sarker, S. Oba, Drought stress effects on growth, ros markers, compatible solutes, phenolics, flavonoids, and antioxidant activity in *Amaranthus tricolor*, Appl Biochem Biotech 186 (2018) 999–1016, https://doi.org/10.1007/s12010-018-2784-5.

[45] U. Sarker, S. Oba, Response of nutrients, minerals, antioxidant leaf pigments, vitamins, polyphenol, flavonoid and antioxidant activity in selected vegetable amaranth under four soil water content, Food Chem. 252 (2018) 72–83, https://doi.org/10.1016/j.foodchem.2018.01.097.

[46] U. Sarker, S. Oba, Drought stress enhances nutritional and bioactive compounds, phenolic acids and antioxidant capacity of *Amaranthus* leafy vegetable, BMC Plant Biol. 18 (2018), https://doi.org/10.1186/s12870-018-1484-1.

[47] U. Sarker, S. Oba, Catalase, superoxide dismutase and ascorbate-glutathione cycle enzymes confer drought tolerance of *Amaranthus tricolor*, Sci. Rep. (2018) 8, https://doi.org/10.1038/s41598-018-34944-0.

[48] U. Sarker, S. Oba, W.F. Alsanie, A. Gaber, Characterization of phytochemicals, nutrients, and antiradical potential in slim amaranth, Antioxidants 11 (2022), https://doi.org/10.3390/antiox11061089.

[49] U. Sarker, M.A. Iqbal, M.N. Hossain, S. Oba, S. Ercisli, C.C. Muresan, R.A. Marc, Colorant pigments, nutrients, bioactive components, and antiradical potential of danta leaves (*Amaranthus lividus*), Antioxidants 11 (2022), https://doi.org/10.3390/antiox11061206.

[50] U. Sarker, S. Oba, S. Ercisli, A. Assouguem, A. Alotaibi, R. Ullah, Bioactive phytochemicals and quenching activity of radicals in selected drought-*Resistant Amaranthus* tricolor vegetable amaranth, Antioxidants 11 (2022), https://doi.org/10.3390/antiox11030578.

[51] U. Sarker, S. Oba, Color attributes, betacyanin, and carotenoid profiles, bioactive components, and radical quenching capacity in selected *Amaranthus gangeticus* leafy vegetables, Sci. Rep. 11 (2021), https://doi.org/10.1038/s41598-021-91157-8.

[52] U. Sarker, S. Oba, Augmentation of leaf color parameters, pigments, vitamins, phenolic acids, flavonoids and antioxidant activity in selected *Amaranthus tricolor* under salinity stress, Sci. Rep. 8 (2018), https://doi.org/10.1038/s41598-018-30897-6.

[53] M.N. Hossain, U. Sarker, M.S. Raihan, A.A. Al-Huqail, M.H. Siddiqui, S. Oba, Influence of salinity stress on color parameters, leaf pigmentation, polyphenol and flavonoid contents, and antioxidant activity of *Amaranthus lividus* leafy vegetables, Molecules 27 (2022), https://doi.org/10.3390/molecules27061821.

[54] U. Sarker, S. Oba, Antioxidant constituents of three selected red and green color Amaranthus leafy vegetable, Sci. Rep. 9 (2019), https://doi.org/10.1038/s41598-019-52033-8.

[55] U. Sarker, M.G. Rabbani, S. Oba, W.M. Eldehna, S.T. Al-Rashood, N.M. Mostafa, O.A. Eldahshan, Phytonutrients, colorant pigments, phytochemicals, and antioxidant potential of orphan leafy *Amaranthus* species, Molecules 27 (2022), https://doi.org/10.3390/molecules27092899.

[56] U. Sarker, Y.P. Lin, S. Oba, Y. Yoshioka, K. Hoshikawa, Prospects and potentials of underutilized leafy Amaranths as vegetable use for health-promotion, Plant Physiol Bioch 182 (2022) 104–123, https://doi.org/10.1016/j.plaphy.2022.04.011.

[57] U. Sarker, S. Oba, Leaf pigmentation, its profiles and radical scavenging activity in selected *Amaranthus tricolor* leafy vegetables, Sci. Rep. 10 (2020), https://doi.org/10.1038/s41598-020-66376-0.

[58] E.J. Jeong, M. Imran, S.M. Kang, M.A. Khan, I.J. Lee, The application of diniconazole and prohydrojasmon as plant growth regulators to induce growth and tuberization of potato, J. Appl. Bot. Food Qual. 94 (2021) 39–+, https://doi.org/10.5073/Jabfq.2021.094.005.

[59] H.T. Kim, S.T. Kim, W.Y. Lee, E.-J. Park, Induction and growth of vegetative stems through in vitro culture of *Gastrodia elata*, Korean J. Med. Crop Sci 21 (2013) 142–147, https://doi.org/10.7783/KJMCS.2013.21.2.142.

[60] T.D. Davis, E.A. Curry, Chemical-regulation of vegetative growth, Crit. Rev. Plant Sci. 10 (1991) 151–188, https://doi.org/10.1080/07352689109382310.

[61] R. Biba, M. Tkalec, P. Cvjetko, P.P. Sefanic, S. Sikic, D. Pavokovic, B. Balen, Silver nanoparticles affect germination and photosynthesis in tobacco seedlings, Acta Bot. Croat. 80 (2021) 1–11, https://doi.org/10.37427/botcro-2020-029.

[62] M. Sarabi, A.S. Afshar, H. Mahmoodzadeh, Physiological analysis of silver nanoparticles and $AgNO_3$ effect to *Brassica napus* L, J. Chem. Health Risks 5 (2015) 285–294, https://doi.org/10.22034/JCHR.2015.544118.

[63] A.T. Harris, R. Bali, On the formation and extent of uptake of silver nanoparticles by live plants, J Nanopart Res 10 (2008) 691–695, https://doi.org/10.1007/s11051-007-9288-5.

[64] Z.M. Almutairi, A. Alharbi, Effect of silver nanoparticles on seed germination of crop plants, J. Adv. Agric 4 (2015) 283–288, https://doi.org/10.24297/jaa.v4i1.4295.

[65] S. Krizkova, et al., Multi-instrumental analysis of tissues of sunflower plants treated with silver(I) ions - plants as bioindicators of environmental pollution, Sensors 8 (2008) 445–463, https://doi.org/10.3390/s8010445.

[66] L. Yin, B.P. Colman, B.M. McGill, J.P. Wright, E.S. Bernhardt, Effects of silver nanoparticle exposure on germination and early growth of eleven wetland plants, PLoS One 7 (2012), e47674, https://doi.org/10.1371/journal.pone.0047674.

[67] E. Navarro, F. Piccapietra, B. Wagner, F. Marconi, R. Kaegi, N. Odzak, L. Sigg, R. Behra, Toxicity of silver nanoparticles to *Chlamydomonas reinhardtii*, Environ. Sci. Technol. 42 (2008) 8959–8964, https://doi.org/10.1021/es801785m.

[68] H.S. Jiang, et al., Silver nanoparticles induced reactive oxygen species via photosynthetic energy transport imbalance in an aquatic plant, Nanotoxicology 11 (2017) 157–167, https://doi.org/10.1080/17435390.2017.1278802.

[69] W. Xing, W. Huang, G. Liu, Effect of excess iron and copper on physiology of aquatic plant *Spirodela polyrrhiza* (L.) Schleid, Environ. Toxicol. 25 (2010) 103–112, https://doi.org/10.1002/tox.20480.

[70] H.S. Jiang, M. Li, F.Y. Chang, W. Li, L.Y. Yin, Physiological analysis of silver nanoparticles and $AgNO_3$ toxicity to *Spirodela polyrhiza*, Environ. Toxicol. Chem. 31 (2012) 1880–1886, https://doi.org/10.1002/etc.1899.
[71] C.H. Foyer, Reactive oxygen species, oxidative signaling and the regulation of photosynthesis, Environ. Exp. Bot. 154 (2018) 134–142, https://doi.org/10.1016/j.envexpbot.2018.05.003.
[72] P.K. Sahu, et al., ROS generated from biotic stress: effects on plants and alleviation by endophytic microbes, Front. Plant Sci. 13 (2022), 1042936, https://doi.org/10.3389/fpls.2022.1042936.
[73] M. Hasanuzzaman, et al., Regulation of ROS metabolism in plants under environmental stress: a review of recent experimental evidence, Int. J. Mol. Sci. 21 (2020), https://doi.org/10.3390/ijms21228695.
[74] F. Abbasi, R. Jamei, Effects of silver nanoparticles and silver nitrate on antioxidant responses in *Echium amoenum*, Russ J Plant Physl 66 (2019) 488–494, https://doi.org/10.1134/S1021443719030026.
[75] Y.K. Mohanta, S.K. Panda, R. Jayabalan, N. Sharma, A.K. Bastia, T.K. Mohanta, Antimicrobial, antioxidant and cytotoxic activity of silver nanoparticles synthesized by leaf extract of *Erythrina suberosa* (Roxb.), Front. Mol. Biosci. 4 (2017) 14, https://doi.org/10.3389/fmolb.2017.00014.
[76] P.A. Tuan, W.T. Park, H. Xu, N.I. Park, S.U. Park, Accumulation of tilianin and rosmarinic acid and expression of phenylpropanoid biosynthetic genes in *Agastache rugosa*, J Agr Food Chem 60 (2012) 5945–5951, https://doi.org/10.1021/jf300833m.
[77] S.Y. Lee, H. Xu, Y.K. Kim, S.U. Park, Rosmarinic acid production in hairy root cultures of Agastache rugosa Kuntze, World J Microb Biot 24 (2008) 969–972, https://doi.org/10.1007/s11274-007-9560-y.
[78] K.T. Desta, et al., The polyphenolic profiles and antioxidant effects of Agastache rugosa Kuntze (Banga) flower, leaf, stem and root, Biomed. Chromatogr. 30 (2016) 225–231, https://doi.org/10.1002/bmc.3539.
[79] W.T. Park, M.V. Arasu, N.A. Al-Dhabi, S.K. Yeo, J. Jeon, J.S. Park, S.Y. Lee, S.U. Park, Yeast extract and silver nitrate induce the expression of phenylpropanoid biosynthetic genes and induce the accumulation of rosmarinic acid in *Agastache rugosa* cell culture, Molecules 21 (2016), https://doi.org/10.3390/molecules21040426.
[80] I.M. Chung, G. Rajakumar, M. Thiruvengadam, Effect of silver nanoparticles on phenolic compounds production and biological activities in hairy root cultures of *Cucumis Anguria*, Acta Biol. 69 (2018) 97–109, https://doi.org/10.1556/018.68.2018.1.8.
[81] I.M. Chung, K. Rekha, G. Rajakumar, M. Thiruvengadam, Influence of silver nanoparticles on the enhancement and transcriptional changes of glucosinolates and phenolic compounds in genetically transformed root cultures of *Brassica rapa* ssp rapa, Bioproc. Biosyst. Eng. 41 (2018) 1665–1677, https://doi.org/10.1007/s00449-018-1991-3.
[82] D.K. Tripathi, et al., Uptake, accumulation and toxicity of silver nanoparticle in autotrophic plants, and heterotrophic microbes: a concentric review, Front. Microbiol. 8 (2017), https://doi.org/10.3389/fmicb.2017.00007.
[83] A. Rastogi, M. Zivcak, D.K. Tripathi, S. Yadav, H.M. Kalaji, M. Brestic, Phytotoxic effect of silver nanoparticles in *Triticum aestivum*: Improper regulation of photosystem I activity as the reason for oxidative damage in the chloroplast, Photosynthetica 57 (2019) 209–216, https://doi.org/10.32615/ps.2019.019.
[84] Z.J. Yu, Q. Li, J. Wang, Y.L. Yu, Y. Wang, Q.H. Zhou, P.F. Li, Reactive oxygen species-related nanoparticle toxicity in the biomedical field, Nanoscale Res. Lett. 15 (2020), https://doi.org/10.1186/s11671-020-03344-7.
[85] A.V. Snezhkina, A.V. Kudryavtseva, O.L. Kardymon, M.V. Savvateeva, N.V. Melnikova, G.S. Krasnov, A.A. Dmitriev, ROS generation and antioxidant defense systems in normal and malignant cells, Oxid. Med. Cell. Longev. (2019) (2019), https://doi.org/10.1155/2019/6175804.
[86] D. Kruszka, A. Sawikowska, R.K. Selvakesavan, P. Krajewski, P. Kachlicki, G. Franklin, Silver nanoparticles affect phenolic and phytoalexin composition of *Arabidopsis thaliana*, Sci. Total Environ. 716 (2020), 135361, https://doi.org/10.1016/j.scitotenv.2019.135361.